

Multi-segment soft robotic fingers enable robust precision grasping

Clark B Teeple¹, Theodore N Koutros^{1,2}, Moritz A Graule¹
and Robert J. Wood¹

Abstract

In this work, we discuss the design of soft robotic fingers for robust precision grasping. Through a conceptual analysis of the finger shape and compliance during grasping, we confirm that antipodal grasps are more stable when contact with the object occurs on the side of the fingers (*i.e.*, pinch grasps) instead of the fingertips. In addition, we show that achieving such pinch grasps with soft fingers for a wide variety of objects requires at least two independent bending segments each, but only requires actuation in the proximal segment. Using a physical prototype hand, we evaluate the improvement in pinch-grasping performance of this two-segment proximally actuated finger design compared to more typical, uniformly actuated fingers. Through an exploration of the relative lengths of the two finger segments, we show the tradeoff between power grasping strength and precision grasping capabilities for fingers with passive distal segments. We characterize grasping on the basis of the acquisition region, object sizes, rotational stability, and robustness to external forces. Based on these metrics, we confirm that higher-quality precision grasping is achieved through pinch grasping via fingers with the proximally actuated finger design compared to uniformly actuated fingers. However, power grasping is still best performed with uniformly actuated fingers. Accordingly, soft continuum fingers should be designed to have at least two independently actuated serial segments, since such fingers can maximize grasping performance during both power and precision grasps through controlled adaptation between uniform and proximally actuated finger structures.

Keywords

Soft robotics, robotic grasping, fluid-driven actuators, gentle grasping, finger design

1. Introduction

Robotic grasping and manipulation often requires some form of online adaptation of grasp strategies. Complex contact interactions between the hand and objects make it challenging to perform grasping without perception, tactile feedback, or otherwise detailed information about the world. In addition, contact interactions can change dramatically depending on the mechanical properties of the object and fingers. Attributes of both structures, such as size, shape, compliance, and surface finish, all play a pivotal role in the stability and precision of the grasping process. Thus, in order to grasp a large range of objects, robots need the ability to adapt their grasps during run-time.

1.1. Traditional robotic grasping

Humans and robots alike use a wide variety of grasps in daily life when performing manipulation tasks (Bullock et al., 2013). In most contexts, grasps can be broadly categorized into power and precision grasps as defined in the

human grasp taxonomy of Cutkosky (1989). Power grasps emphasize stability, usually involve enveloping the object, and are often accomplished using multiple points of contact between the object and the surfaces of the fingers and palm. This definition of power grasping can be abstracted for robotic hands with less anthropomorphic designs to involve multiple points of contact between each finger and the target object, leading to an enveloping grasp. Precision grasps on the other hand, such as fingertip or pinch grasps, involve more focus on applying small forces and enabling such capabilities as dexterous manipulation. For robotic hands,

¹School of Engineering and Applied Sciences, Harvard University, Cambridge, MA, USA

²ETH-Zurich, Swiss Federal Institute of Technology, Zurich, Switzerland

Corresponding author:

Clark Teeple, Harvard Microrobotics Laboratory, Harvard University, Cambridge, MA 02138, USA.
Email: cbteeple@g.harvard.edu

precision grasps usually involve only one contact point per finger.

Traditional rigid robotic hands accomplish grasping adaptability by increasing the number of actuated degrees of freedom and relying on complex control strategies to coordinate them. Several examples of highly articulated robotic hands exist, and an overview is included as part of Amend and Lipson (2017). Most high-dimensional robotic hands are anthropomorphic in design, and usually include at least one actuator for each finger joint. Examples include the Utah/MIT dexterous hand (Jacobsen et al., 1986), the ShadowRobot Shadow hand (Kochan, 2005), the Robonaut 2 hand (Bridgwater et al., 2012), and the SimLab Allegro hand by Bae et al. (2012). Each of these hands have 16–20 actuators, and the Shadow hand can be configured with up to 40 actuators. While highly dexterous, the complexity of control needed to coordinate these hands is usually large, and unnecessary for many grasping tasks.

1.2. Compliance in robotic grasping devices

A paradigm shift toward under-actuated fingers with built-in compliance has emerged as a way to embody a robot hand with structural adaptability during grasping, without complex control. Structural compliance enables passive adaptation to object shapes without explicit knowledge of the object or environment. For example, the Robotique two-finger gripper family uses a single actuator, but can still adapt between a parallel plate grasp and an enveloping power grasp (Robotiq, 2019). Using carefully designed kinematics, joint limits, and joint compliance, this rigid hand adapts its grasp passively based on where and how the force vectors are applied to the plates. Achieving similar kinematic behavior, the Velo Gripper (Ciocarlie et al., 2014) utilizes tendon-driven fingers to passively adapt the grasp in a more-compact mechanism. Furthermore, the Pisa/IIT Soft Hand (Catalano et al., 2014) utilizes joint compliance and mechanical coupling between fingers as adaptive grasping synergies to achieve close to human performance with only four actuators.

While joint compliance in planar pin joints enables robust finger adaptation during grasping, three-dimensional compliance extends robustness to uncertainty. The SDM Hand (Dollar and Howe, 2010), for example, uses compliant finger flexures as joints, allowing for small off-axis finger motions during grasping. With the addition of sensing and other design changes, the iRobot-Harvard-Yale (iHY) hand by Odhner et al. (2014) achieves high passive compliance in actuated directions to enable robust power grasping, while retaining a small off-axis compliance for precision grasping.

Building on the successes of simple, yet robust passive adaptation, others have chosen to focus on modulation of joint stiffness through additional actuators or impedance control. For example, the BarrettHand grasper (Townsend, 2000) and the SRI Hand (Aukes et al., 2014) use clutches in the joints to lock them in place. This enables passive

adaptation to object shape, and strong grasps when the clutches are engaged. Conversely, the DLR Hand II (Butterfaß et al., 2001) and recently CLASH (Friedl et al., 2018) achieve fingertip stiffness modulation through impedance control and a clever differential drive mechanism. This allows on-the-fly stiffness control without additional actuators.

In an orthogonal approach to compliant grasping, local compliance at the fingertips is utilized through finger pads rather than compliant fingers or joints. For example, Maruyama et al. (2013) developed deformable fingertips that can interact gently with objects first, then increase their stiffness as they deform. More recently, McInroe et al. (2018) developed a similar soft fingertip that uses pneumatic actuation to apply forces to objects, while also being capable of measuring the fingertip's complex deformation. In addition, compliant fingertips have the potential to improve the stability of a grasp due to increased contact area and restoring forces according to Cutkosky and Wright (1986). However, compliant fingertips only ensure gentle interactions with objects directly at the fingertips.

1.3. Soft robotic hands

Recently, more focus has been placed on building robotic hands that can safely and gently interact with their environments. This shift in application goals has given rise to soft robotic hands, where both the finger structure and contact surfaces are made of compliant materials (Rus and Tolley, 2015). Rubbers, fabrics, and foams are used to build actuators that minimize the risk of damage, especially when interacting with delicate targets (Hughes et al., 2016; Majidi, 2014). In addition, passive compliance of soft fingers reduces the control complexity required to robustly grasp objects (Polygerinos et al., 2017; Rus and Tolley, 2015). However, what soft robots gain in adaptability, they often lose in strength and precision (Shintake et al., 2018).

Soft robotic hands or grippers are typically well-suited to grasp unknown, irregularly shaped, or delicate objects. This can also translate to better handling of uncertainties in object pose that arise from vision and other sensory systems. For example, Ilievski et al. (2011) demonstrated a soft gripper with a single pneumatic input capable of performing grasps on objects with minimal sensitivity to position errors. Brown et al. (2010) developed a universal jamming gripper capable of grasping a wide array of object shapes. In an interesting application, Galloway et al. (2016) designed and deployed a soft hand to perform sampling of delicate marine life in the deep sea, one of the most challenging environments to operate in. Furthermore, Deimel and Brock (2016) built a dexterous soft hand, the RBO Hand II, capable of performing all but two grasps in the Feix taxonomy (Feix et al., 2009).

While most soft hands can perform excellent power grasping due to passive compliance, they typically have trouble grasping small objects using precision grasps. During deep-sea exploration, the gripper built by Galloway

et al. (2016) could withstand up to 17 N applied to the object during a power grasp with two opposing fingers, but relied on caging animals that were smaller than the minimum power grasping size. Using a jamming gripper, enveloping grasps can be used for small objects, but can only be performed by pressing objects against a surface (Brown et al., 2010). With more dexterous soft hands such as the RBO Hand II by Deimel and Brock (2016), the majority of successful grasps performed were power grasps. While the RBO hand is capable of withstanding forces up to 8 N, grasp stiffness was a main limitation due to the large finger compliance. In another example, Zhou et al. (2017) presented a new soft hand capable of very robust power grasps, but with no characterization of precision grasp performance.

The focus of recent work in soft grasping has been on performing power grasps, without much emphasis on precision grasps. For example, the Pisa/IIT Soft Hand (Catalano et al., 2014) makes use of postural “soft” synergies that describe principle components of hand motions over a set of grasping tasks. In another study, O’Brien et al. (2018) demonstrate how soft structures can be used to passively adapt between high-force and high-speed operation modes. However, precision grasps were not the focus of either of these studies. Other recent studies of soft finger design focused entirely on power grasps, using simulation (Deimel et al., 2017) and experimentation (Knoop et al., 2017). Furthermore, one recent study has been presented by Vogt et al. (2018) where adding a passive extension to soft fingers enabled them to perform pinch grasps. However, the extension would likely interfere with power grasp operation.

Finally, the effect of adding multiple bending segments to soft fingers has not yet been explored for precision grasping. While Deimel and Brock (2013), Zhou et al. (2017), and Zhou et al. (2018) built soft fingers with more than one serial segment, all three studies focus on exploring the effect of their hand designs on power grasps. Zhou et al. (2017) in particular found that the pullout force can be improved if fingers with two segments are actuated in a particular way. However, to date, precision grasping with soft fingers remains an open and relatively unexplored design space.

1.4. Overview

In this work, we show how simple, conceptual design rules can be used to design soft robotic fingers capable of excellent precision grasping without sacrificing power grasping performance. We present three main contributions: (1) a conceptual analysis of compliance and finger shape during grasping, which suggests that soft fingers should have at least two serial bending segments; (2) an empirical study of grasping performance comparing this two-segment finger design with uniformly actuated fingers; and (3) experimental validation showing that fingers with two independently actuated serial segments can achieve excellent precision and power grasps.

We first present a conceptual analysis of precision grasping with multi-segment soft fingers based on compliance and local finger shape. This high-level analysis suggests that grasps are more stable when contact with the object occurs on the side of the finger (a pinch grasp) rather than the fingertip. In addition, achieving a pinch grasp with soft continuum fingers requires at least two independent bending segments each, but only requires actuation in the proximal segment. Furthermore, we explore the effect of the relative lengths of finger segments on pinch grasping performance.

Next, we empirically evaluate the grasping performance of the two-segment, proximally actuated finger design compared to widely used uniformly actuated fingers. Performance is evaluated using several metrics: the acquisition region, object size range, rotational stability, and robustness to external forces. We confirm that the proposed proximally actuated finger design is capable of higher-quality precision grasping than fingers with a uniformly actuated design, and we show the tradeoff between power grasping strength and precision grasping capabilities as a function of segment length. However, power grasping is still best performed with uniformly actuated fingers. Thus, compromises in performance would need to be made if one single finger structure were to be chosen for each finger.

Finally, we show that adaptation between uniformly actuated and proximally actuated finger structures using two independently actuated serial segments (as shown in Figure 1) can achieve the best possible performance during both types of grasps, and can be implemented with only a limited increase in control complexity.

2. High-level finger design principles

To understand how the number of independent serially linked segments in a soft finger affects its ability to perform robust grasps, we can build a conceptual argument around compliance and geometry at the contact point. Finger compliance directly affects fingertip motion when external forces are applied to the object. In addition, the shape of the finger and object at the contact point can be used to determine the sensitivity of object motion to fingertip motion. Combining knowledge of a finger’s compliance ellipse with the local fingertip shape provides useful insight into the stability of that grasp, which can ultimately be used to judge the quality of the finger design.

2.1. Fingertip compliance

The compliance of any mechanical structure or linkage can be represented by the deflection of some point of interest in response to unit force applied at all angles, resulting in an elliptical region. This so-called compliance ellipse has been used to study human arm and finger function to visualize compliance in human extremities (De and Tasch, 1996; Hajian and Howe, 1997; Mussa-Ivaldi et al., 1985). Compliance ellipses also form the basis of impedance

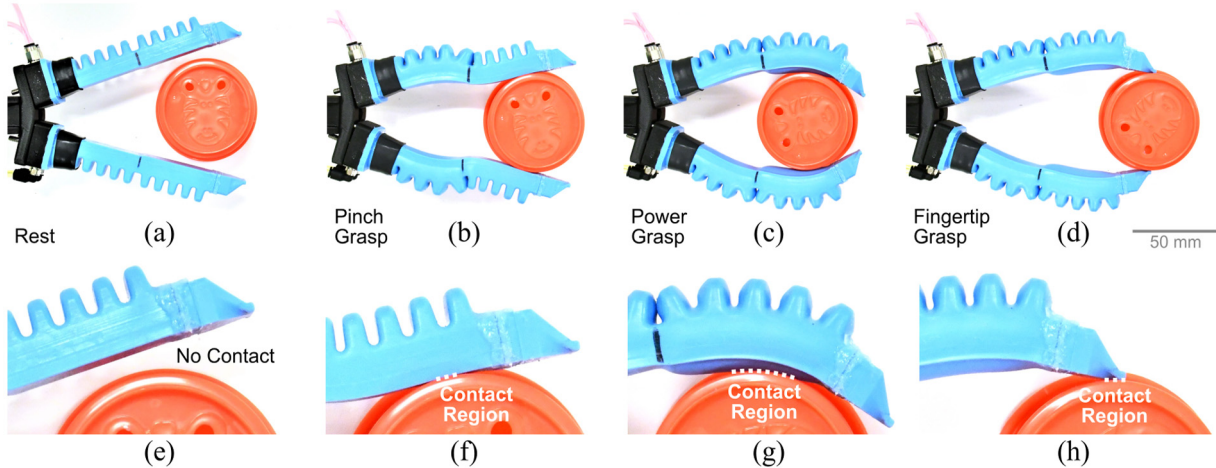


Fig. 1. Our planar hand prototype with two co-planar segments per finger grasping a cup of 55 mm diameter. The hand is shown (a) at rest, (b) performing a pinch grasp with the sides of the fingers, (c) performing a power grasp, and (d) performing a fingertip grasp. Enlarged views of fingers in (a), (b), (c), and (d) are shown in (e), (f), (g), and (h), respectively.

control for robotic systems (Hogan, 1985), where a desired endpoint stiffness can be achieved through joint control. In addition, Lim and Tanie (2000) showed that designing the compliance ellipse at many points along the whole body of a mobile robot can improve the safety of human–robot interactions. Thus, it is natural to apply the same arguments to aid in the design of robotic fingers.

Designing fingers to achieve a desired tip-compliance ellipse (an ellipsoid in three dimensions) has proven to be a simple, yet effective method for highly under-actuated systems. For example, De and Tasch (1996) used impedance control to achieve a similar endpoint compliance ellipse to the human finger based on empirical measurements. In addition, Gravagne and Walker (2002) showed that the compliance ellipsoid of a continuum manipulator can be used to understand complex deflections under different tip loads. Finally, Odhner et al. (2014) used analysis of fingertip compliance when designing the flexure-based fingers of the iHY hand, with the goal of aligning the major axis of the compliance ellipsoid normal to the fingertip surface. By examining the compliance ellipsoid of a set of generic soft fingers with multiple segments, we can understand how to best utilize control inputs for robust grasping.

2.2. Fingertip curvature

Geometric analysis of how fingertip shape affects the rolling motion of an object can be used to gain some notion of the stability of a fingertip grasp. Cutkosky and Wright (1986) developed this analysis by investigating how several mechanical aspects of a finger affect the rotational stability of a grasp (i.e., how an infinitesimal rotation of the object affects stability). They found that the stability of a planar fingertip grasp increases as a function of both the radius of curvature and stiffness of the finger at the contact point. Furthermore, they found that with a sufficiently large radius

of curvature, the grasp stability is infinitely stable regardless of finger stiffness. While this analysis assumes rigid fingertips, they note that the trends remain the same for soft fingertips.

Based on the insights from Cutkosky and Wright (1986), Montana (1992) developed a description of grasp stability that agrees with this intuition. Under this framework, stability is increased with larger radii of curvature of both the object and fingertip. In addition, mechanical properties such as normal forces and viscoelasticity were found to only affect the stability of marginally stable grasps. For example, increased viscoelasticity at the contact point was found to result in increased stability. This analysis again assumes perfect rolling contact, and looks at rotational stability, but is useful nonetheless to understand how soft fingers can be best utilized to perform robust precision grasps.

2.3. Precision grasping with soft fingers

To design fingers that can perform high-quality precision grasping, the above analyses suggest the finger should have low compliance and small fingertip curvature at the contact point. Through examination of the local shape and compliance of soft fingers, we find that the placement of contact points on the side of the finger enables pinch grasping with a dramatic improvement in stability compared to fingertip grasps. The subsequent analysis is performed in the planar case ignoring the effects of gravity, but the resulting design rules can be extended to real-world grasping in a straightforward way (as presented in the Section 7).

2.3.1. Single uniformly actuated segment. As a baseline, let us first explore precision grasping using fingers with a single uniform bending segment. As the fingers are actuated, they first have uniform curvature over the whole length, then contact with an object causes non-uniform

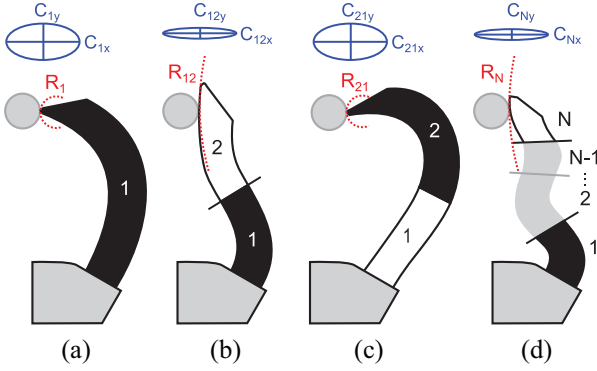


Fig. 2. The shape of soft continuum fingers as they perform precision grasps with different numbers of bending segments. (a) One uniformly actuated bending segment yields a fingertip grasp with small radius of curvature and larger anterior (C_y) compliance. (b) Two segments with only proximal actuation enable a pinch grasp with a much larger radius of curvature and smaller compliance. (c) Two segments with only distal actuation yields a fingertip grasp similar to that of a single uniformly actuated bending segment (d) More than two segments yields the ability to control fingertip orientation separately from position, with more options for actuation inputs to produce the desired pinch grasping configuration.

curvature with lower curvature at the proximal ends. This decrease in proximal curvature is due to the long moment arm over which the contact force acts. The result is that during a grasp, the ends of the fingertips contact the objects, as shown in Figure 2(a). Most examples of existing soft robotic fingers exhibit this behavior (Deimel and Brock, 2016; Galloway et al., 2016; Morrow et al., 2016).

The placement of forces on the fingertips results in grasps with low stability. First consider the local shape of the fingertips. While the fingertip curvature is highly variable, many designers choose to use pointed fingertips to improve power grasping against surfaces (Deimel and Brock, 2016; Morrow et al., 2016). However, pointed fingertips result in very high curvature (small radius) at the contact point during fingertip grasps, causing large object deflections from relatively small fingertip deflections. Furthermore, according to Cutkosky and Wright (1986), the grasp stability is a function of the object's curvature. On top of this, the fingertip compliance in the axis normal to the palm's surface is usually relatively large, causing large fingertip deflection from relatively small forces on the object.

2.3.2. Actuated proximal segment, passive distal segment. Now consider a finger that has two uniform bending segments of equal stiffness, but only the proximal segment (closest to the base) can be actuated. In this case, during grasping the passive distal segment can perform a passive backward bend in order to balance forces on the object. Zhou et al. (2017) utilized this phenomenon to grasp objects larger than the opening width of the fingers.

During a precision grasp, the passive bend allows the contact points to be moved from the fingertip to the inside edge of the finger to form a pinch grasp given appropriate object position, as shown in Figure 2(b).

Grasping with the sides of the finger results in more-stable pinch grasps. Compared to the case of a fingertip grasp, the local geometry at the contact point has much higher curvature and lower compliance in the direction normal to the palm. In fact, the object contacts the finger on a flat surface of approximately zero curvature (infinite radius), meaning grasp stability should have low dependence on object curvature and hand placement inaccuracies. Furthermore, grasp stability (and robustness) becomes mostly dependant on friction between the finger and object because the finger compliance in the direction normal to the palm is much lower. This approximates grasping with a parallel-jaw gripper.

2.3.3. Passive proximal segment, actuated distal segment. Next, consider flipping the two-segment configuration, where only the distal segment can be actuated. In this actuation scheme, the fingertip ends up touching the object and bends the passive proximal segment backward, as shown in Figure 2(c). Similar to a single uniformly actuated segment, contact at the fingertip yields poor grasp stability due to the large fingertip curvature and high compliance.

2.3.4. More than two segments. In a final case, consider a finger that has more than two bending segments. During a pinch grasp, we assume the object will only touch the finger at a single point. Even with only three segments, the finger now has a family of input configurations that can place the contact points on the inside edge of the finger, as shown in Figure 2(d). While an increase in the workspace of the finger would likely enable interesting functionality, we are focused on the two-segment case since that is the minimal configuration where desirable pinch grasping behavior can occur with the sides of the fingers.

2.3.5. Relative stiffness of finger segments. While it may be possible to enable the desired placement of contact points with only one bending segment of non-uniform stiffness, we restrict the focus of this work to uniform bending segments for simplicity. Prior work in this area from Knoop et al. (2017) shows that non-uniform stiffness can be used to tune the contact pressure a soft finger applies at each point along its contact surface. However, the impact of these tuned contact-pressure profiles on grasping performance has not been evaluated in detail. In addition, there are likely inherent compromises in grasping performance when designing one mechanism to passively adapt between robust pinch grasping and strong power grasping. Rather than attempting to search a potentially large design space, we focused on using fairly simple sub-components (serially

linked uniform bending segments of equal stiffnesses) with simple relationships between actuation pressure and free curvature.

2.3.6. Relative lengths of finger segments. To gain a high-level conceptual understanding of how the relative lengths of finger segments affect precision grasping performance, we can abstract the two-segment fingers as two serially connected cantilever beams. Assuming a symmetric grasp, we can further simplify the grasp and look at only one finger. During a grasp, each finger segment can potentially have a single point load (from contact with the object) and an internal moment (from actuation pressure). With the proximal segment rigidly fixed to mechanical ground (the palm), the distal segment is joined serially with the proximal beam at the “connection point.” The following discussion is limited to a contact force applied only in the distal segment, which is the case in many successful pinch and power grasps.

First, consider the effect of lengthening the proximal segment. The deflection and bending angle at the “connection point” increase with increasing actuation torque and length of the proximal actuator. This deflection and angle define the neutral position of the distal segment. Next, for an object with a fixed relative position and size, the position of the contact point on the distal segment is constrained. The deflection of the distal segment at the contact point therefore increases with increasing torque and length of the proximal actuator. Thus, for a constant actuation torque in the proximal segment, the contact force on the object increases as the proximal segment gets longer.

Similarly, the stiffness of the unactuated distal segment, and thus the contact force, increases with decreasing distal segment length. Furthermore, keeping overall length constant, an increase in the length of one segment directly results in a decrease in length for the other segment.

Since these two effects are additive, a smaller distal length fraction generally enables higher contact forces on the object. Finally, higher contact forces lead to increased frictional forces assuming a constant friction coefficient between fingers and the object. Thus, we expect grasps to have increased robustness to external forces with proximally actuated finger structure with decreasing distal length fraction.

2.4. Power grasping with soft fingers

As detailed in Section 1, strong power grasping has been achieved in numerous studies, and can be robustly achieved using fingers composed of one uniformly actuated bending segment. Therefore, to achieve the best possible grasping performance for power and precision grasps using soft continuum fingers, we can see that two fundamentally different finger structures are required. For the strongest possible power grasp, the obvious choice is the more-traditional finger design with one uniformly actuated bending segment. Conversely, to achieve the most-stable precision grasping,

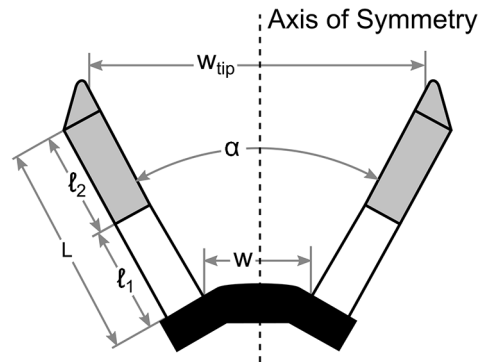


Fig. 3. Schematic diagram of our planar soft-robotic hand prototype. Each finger has two bending segments of lengths ℓ_1 and ℓ_2 . Two fingers are mounted to a palm with a width of w and an angle of α between them.

fingers need at least two bending segments, but only the proximal segment needs to be actuated. In the following sections, we empirically investigate the tradeoffs in grasping performance that arise from each finger structure

3. Designing a prototype soft hand

To illustrate the concepts explored in the previous section, we designed and built a soft robotic hand capable of interacting with objects in a plane. The hand consists of two fingers, each with two independent co-planar bending segments. The fingers are mounted on a rigid palm with some distance and angle between them, as shown in Figure 3. The following sections detail the design choices made and fabrication methods used to build a robust grasping system we can use to test our claims.

3.1. Designing modular two-segment fingers

Several criteria were taken into account when designing the fingers of our soft robotic grasping system. For simplicity, we limit the fingers to two serial bending segments. Two segments is the minimal configuration needed to enable placement of contact points on the side of the fingers, as discussed in the previous section. These segments should also have equal passive stiffness in order to approximate a single bending segment when equal actuation inputs are applied to both segments. In addition, the relative lengths of the two segments is a parameter of interest, so this should be easy to choose during construction. Finally, the fingertip shape should be consistent with other soft fingers designed for power grasping so as to preserve power grasping performance.

To address these design criteria, several key choices were made during the design process. First, the fingers utilize bellows-style pneumatic bending actuators as used in Galloway et al. (2016). Each finger is split into two independently actuated serial segments, as shown in Figure 4(a), with the ability to control the relative lengths

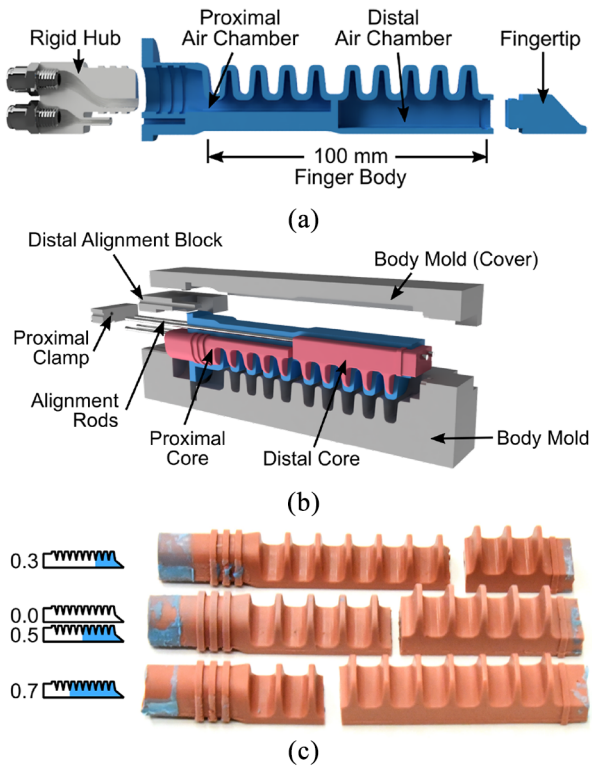


Fig. 4. (a) Each soft finger is composed of a silicone skin and fingertip (both made out of Smooth-Sil 950), and a rigid hub at its base. The body of the finger contains two bellows-style pneumatic bending segments. (b) To fabricate a finger, we use a four-part mold made of 3D-printed resin (VeroClear RGD 810), as well as two soft silicone cores (Elastosil 4061, Wacker). (c) The soft cores can be trimmed to length to generate fingers with different segment lengths.

of the two segments at design-time. We keep each finger's workspace free of tubing by routing pneumatic connections through one proximal hub on each finger. However, internal routing of pneumatic lines required extra thickness in the proximal actuator wall. To ensure the bending stiffness of both segments is roughly equal, extra thickness in the proximal actuator walls was placed near the neutral bending axis. Finally, we used wedge-shaped fingertips since this shape is commonly employed for better power grasping against surfaces (Morrow et al., 2016).

In addition to addressing explicit design goals, several aspects of the finger design space were held constant for simplicity. The most critical constant parameter is the overall length of the fingers, chosen to be of the order of 100 mm so as to be roughly the length of a large human finger. Differences in the segment lengths with respect to each other are controlled while keeping the overall finger length constant. In addition, we expect the stiffness of each segment (relative to actuation pressure) to contribute directly to the shapes that fingers form. However, while we would expect these fixed parameters to shift grasping performance and affect the magnitude of tradeoffs in the performance

metrics, we would not expect them to fundamentally alter the results when comparing fingers with two actuated segments to fingers with one uniformly actuated segment.

3.2. Fabricating two-segment fingers

The fabrication process for our two-segment soft fingers involves a variation on the molding techniques described by Galloway et al. (2016), as well as coupling with rigid 3D printed hubs for fluid and structural connections. All molds were 3D printed on an Object Connex 500 printer (VeroClear material, Stratasys). All hubs were printed either on an Object Connex 500 printer with VeroBlue material or on a Markforged Onyx One printer in Nylon with chopped carbon fiber (Onyx Material, Markforged).

The interior geometry of the finger is created using two soft-bodied cores. These cores are made using a typical molding process. First, Elasto-Sil M-4601 (Wacker) is mixed, then poured into both sides of the mold. Next, the mold halves are de-gassed in a vacuum chamber, and steel alignment rods (2 mm diameter) are placed. The mold is then clamped together and placed in a 65°C oven for 3 hours until fully cured.

The body of the finger is created by a four-part mold, as shown in Figure 4(b), which is constant across all relative segment lengths. The relative lengths of the finger's two segments are instead chosen by adjusting the lengths of the soft cores before molding, as shown in Figure 4(c). To build the body, the mold is filled halfway with Smooth-Sil 950 (Smooth-On Inc.). After degassing, the proximal soft core (with alignment rods) is inserted into the mold, then fixed with the proximal clamping piece. Next, the distal alignment piece is placed, followed by the distal soft core. More silicone is subsequently poured to cover the cores completely. The mold is then clamped together between two aluminum plates and placed in a 65°C oven for 3 hours until fully cured.

To plug the distal end of the finger, a fingertip is attached. The fingertip is created using Smooth-Sil 950 and the same basic molding process as the soft cores (without alignment rods). The piece is then attached to the distal segment using interlocking features and silicone adhesive (Silpoxy, Smooth-On Inc.).

Finally, a rigid hub is attached to the proximal side of the finger body to enable air delivery. The holes created by the alignment rods for the distal core also act as fluid channels to deliver air to the distal segment. Thus, both fluid connectors can be located in the proximal hub. The hub is fixed to the skin using interlocking features and Silpoxy. Once the adhesive is cured, heat-shrink tubing is wrapped around the proximal end of the finger to ensure no leaks.

3.3. Designing a rigid palm

For all subsequent testing and analysis, only grasping in a plane will be considered since it directly illustrates the benefits of including multiple bending segments in soft fingers.

To design a suitable rigid, planar palm, two competing design criteria were considered. Grasping objects of zero width is only possible if the distal parts of the actuators come into contact. However, the resting position of the actuators should also have a wide opening angle to be able to grasp comparatively larger objects (see Figure 3).

Thus, two design parameters are free to be chosen: the width at the base, w , and the angle between fingers, α . Since the actual shape of the soft fingers can be complex during a grasp, several candidate palms were built and a single palm was chosen based on empirical testing (see the following section). All candidate palms were 3D printed on an Object Connex 500 printer with VeroBlue material, and the final design was printed on a Markforged Onyx One printer in Nylon with Onyx Material.

4 Characterizing fingers and palm

Characterizing the kinematic and mechanical properties of the fingers is critical before we can understand the grasping behavior of the hand as a whole. We first defined two actuation modes that allow the fingers to exhibit fundamentally different behavior while grasping. We then characterized the curvature and blocked force responses of individual segments under actuation pressure, and evaluate the maximum pressure before failure to determine a pressure operating point. We also measured the stiffness of each segment to confirm they are similar. Sufficient similarity between both segments allows our soft fingers to achieve finger motion similar to a single bending segment when equal pressures are applied to both segments. Finally, we use all of this information to design the rigid palm to be used for robust grasping.

4.1. Actuation modes replicate finger structure

To simplify the combinations of actuation inputs, we restrict our focus to two actuation modes that enable the fingers to replicate two fundamentally different finger structures, as shown in Figure 5. In the first actuation mode, (“*proximal-actuation*” mode), only the proximal segment is actuated while keeping the distal segment passive. In the second actuation mode, (“*uniform-actuation*” mode), both segments are driven with equal pressure so that the actuated region spans the entire length of the finger. This enables our prototype fingers to achieve the same behavior as fingers built with a single uniformly actuated segment. Thus, using only pressure control, our two-segment fingers can be used to investigate how grasping behavior differs depending on finger structure.

4.2. Functional evaluation of fingers

We performed a series of experiments on several fingers to determine the response of individual segments to input pressure. To control the pressures independently in each segment of the fingers, we used a custom pneumatic

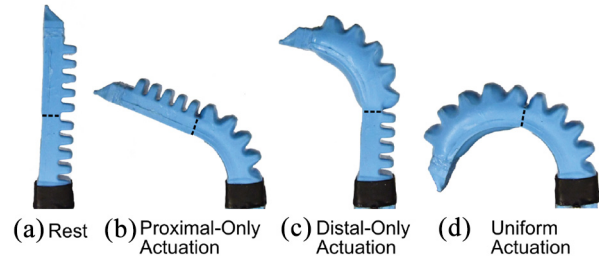


Fig. 5. Fingers with two segments can be actuated a number of ways. A finger is shown (a) at rest, (b) with *proximal-only* actuation, (c) with only distal actuation, and (d) with equal pressure in both segments (*uniform*-actuation).

pressure control system with an accuracy of 1.4 kPa. For each of the four channels, the controller enables smooth control of output pressure around a setpoint, and execution of arbitrary pressure trajectories in real time. A more detailed description of our pressure control system can be found in the Supplementary Material.

We first recorded the change in curvature as a function of input pressure. We performed this experiment on the proximal and distal segment as well as for the whole actuator. The actuation pressure is increased from 0 to 138 kPa in 13.8 kPa increments, and the resulting curvature is measured by hand from photographs, as discussed in the Supplementary Material. The average curvature ranges from 0 (flat segment) to 32.24 and 28.54 m⁻¹ for the proximal and distal segment, respectively, as shown in Figure 6(a). As the pressure reaches 100 kPa, the distal segment’s curvature does not show any further significant increase. Overall, the relationship between input pressure and curvature is fairly similar between segments, with a maximum of 22% difference in curvature occurring around 70 kPa.

Furthermore, to evaluate the limitations in actuation, both segments of three separate fingers were inflated until they failed by rupturing. The recorded burst pressures were 240 ± 14 kPa for the proximal segments, and 186 ± 20 kPa for the distal segments. Failures occurred in the bellows sections of both segments. To prevent structural failures during normal operation, we choose to use a maximum actuation pressure of 100 kPa.

Next, blocked force as a function of actuation pressure was measured for both segments using an Instron 5544A. Fingers are clamped in a vise and placed under the Instron, as shown in Figure 7(b). The rigid hub is clamped when characterizing the proximal segment, and the finger itself is clamped when measuring the distal segment. Next, a thin plastic sheet is clamped in the jaws of an Instron machine to ensure a small contact point with the finger. The pressure is then applied and the resulting vertical blocked force is measured, as shown in Figure 6(b). The difference in the slopes between the proximal and distal segments is likely due to the difference in the cross-section of the air chambers, which was discussed earlier in Section 3.1. Overall,

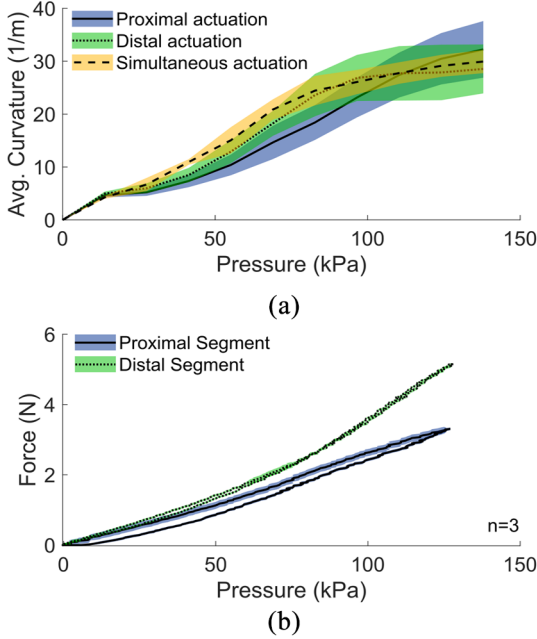


Fig. 6. (a) The curvature of each finger segment as a function of applied actuation pressure is recorded every 13.8 kPa up to 138 kPa. (b) The blocked force as a function of applied actuation pressure shows only slight hysteresis over the 0–138 kPa range. The mean and standard deviation of $n=3$ trials is shown.

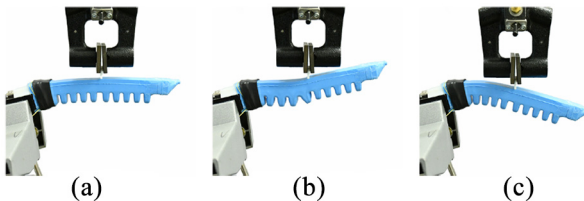


Fig. 7. Characterization of the stiffness and blocked force for each segment was performed on an Instron system. (a) The finger is clamped in a vise. (b) Blocked force is measured by applying input pressure and measuring the resulting force. (c) Segment stiffness is measured by deflecting the finger by 10 mm while measuring the force. In both cases, the finger presses against a thin plastic sheet.

the relationship between input pressure and blocked force has a similar shape for both segments.

Finally, the stiffness of each bending segment was characterized by applying small deflections at the tip of the segments and recording the resulting force. First a finger is clamped in a vice and placed under an Instron machine using the same procedure as the blocked force tests, as shown in Figure 7(c). Next, a thin plastic sheet is clamped in the jaws of an Instron machine, and used to apply 10 mm of deflection to the tip of the segment. The resulting force is measured using a 10 N load cell. Given the linearity of the force-deflection curves, the stiffness is calculated as the slope of this line, as shown in Table 1.

Table 1. Bending stiffness of individual bending segments of fingers. The mean and standard deviation are reported for $n=3$ trials of each sample.

Finger sample	Stiffness (N/m)	
	Proximal	Distal
#1	84.2 ± 0.8	66.3 ± 0.2
#2	83.1 ± 0.4	92.4 ± 3.4
#3	75.3 ± 0.3	50.4 ± 0.2
#4	70.4 ± 1.0	57.9 ± 0.9
Average	78 ± 6	58 ± 8

For all of the four fingers characterized, the stiffness of the distal segment was within 33% of the proximal stiffness, with differences as low as 10%. This discrepancy in stiffness is caused partially by the mechanical design of the finger, since the wall of the proximal segment at the inside of the bend is thicker to accommodate the distal air supply channels.

To create the fairest comparison between finger structures with uniform actuation versus proximal-only actuation, an important design goal was to ensure that each finger can achieve both structures through differences in actuation. The “proximally actuated two segment” structure is trivial to implement by design. However, given the small magnitude of the difference in segment stiffness, combined with the similar bending and blocked force responses for both segments, we confirm our assumption that our fingers can behave like a single bending segment through *uniform actuation*.

4.3. Finding a suitable palm angle

Choosing an appropriate angle between fingers (palm angle α) and palm width, w , is critical to allow for robust pinch grasps while also maximizing the largest attainable object diameter. As our soft fingers are limited to 100 kPa input pressures to prevent actuator failure, the resulting curvature is also limited. Thus, the geometry of the palm must ensure the fingers touch when only the proximal segment is actuated, while simultaneously achieving the widest possible distance between fingers at rest.

To maximize the potential for fingers to touch under *proximal-only* actuation, the palm width was chosen to be relatively short (15 mm). This short distance between the bases of each finger could potentially affect the overall robustness of power grasps. In fact, many other hand designs (including humans) utilize the palm as a contact surface during power grasps. However, our primary goal is to compare finger designs during both precision grasping and power grasping, so the palm width is less important.

To find the finger angle that meets these criteria under actuation constraints, we evaluated the contact area at the fingertips under a proximal actuation of 100 kPa on several prototype palms. Five palms were tested, ranging from an angle of 60° to 20° with a constant base width of 15 mm, as

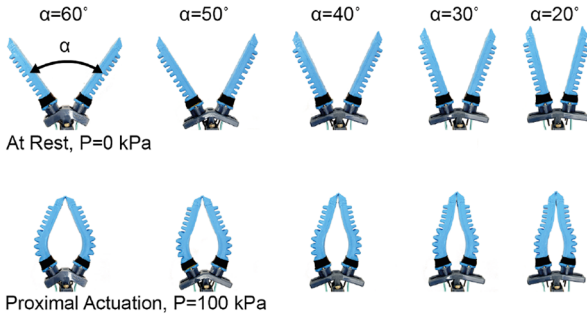


Fig. 8. Several palms with varying angles were evaluated at rest and with the proximal segment pressurized to 100 kPa. We chose an opening angle of 30° , as this is the largest angle where the fingers achieve the non-zero distal contact area when actuated.

shown in Figure 8. Ultimately, an angle of 30° between fingers was chosen due to the larger distal contact area under proximal-only actuation.

5. Characterizing grasping performance

For each pair of two fingers and the final palm design, we evaluated the effect of actuation modes on several relevant grasping metrics. We first evaluated the effect of hand placement (with respect to the object) on the type of grasp performed. These tests also enabled evaluation of the range of object diameters the hand can grasp. We then explored the hand's robustness to external forces. Finally, we measured the finger compliance during grasping. All tests were performed for both actuation modes.

5.1. Hand placement

For our soft fingers, the type of grasp performed is determined by the placement of the hand with respect to the object, and the actuation mode used. To evaluate this effect, we performed a series of grasp attempts on a set of cylindrical objects to determine the ranges of centering positions that cause power grasping, pinch grasping, or failure. In addition, these experiments also yield the region of acquisition for different objects along the axis normal to palm.

To perform reliable grasping at precisely controlled positions, the hand was mounted to one of two Cartesian positioning systems: either a custom-built three-axis CNC gantry, or a UR5e 6DOF robot arm (Universal Robots, Denmark), each with a positioning accuracy of better than 1 mm. For the gantry system, GCODE commands were used to command hand positions, while for the robot arm, MoveIt! (Chitta et al., 2012) was used for motion planning. Robot Operating System (ROS; see Quigley et al. (2009)) was used to coordinate motion and hand pressure control for both systems. To maintain a symmetric grasp, we actuate the homologous segments of both fingers with the same actuation signals, assuming symmetry between



Fig. 9. Objects used for grasping characterization. Objects are part of the YCB object set except the two bolts, the syringe, and the tube grommet.

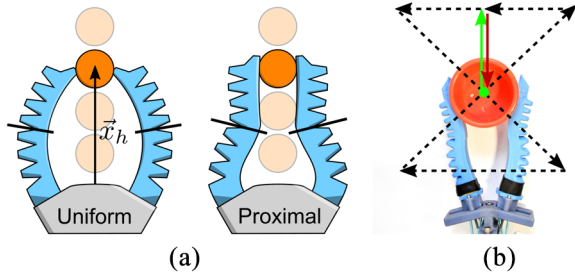


Fig. 10. Experimental setup for exploring grasp types over a range of centering offsets (x_h) and object diameters (D). (a) The object is grasped with some centering offset, then (b) the hand is moved in a zig-zag pattern to check whether the grasp is successful.

ingers. Pictures of both experimental setups are shown in the Supplementary Material.

The set of objects used in this study was chosen to reach both ends of the size spectrum that our soft hand can grasp. A set of 11 cylindrical objects ranging from 2.2 to 116 mm in diameter were chosen. Most of the objects belong to the Yale–Carnegie Mellon–Berkeley (YCB) object set (Calli et al., 2015), and a few extra objects were added to fill in gaps in the smaller size range, as shown in Figure 9). The actual objects used are discussed in the Supplementary Material.

A typical test for a given object involves grasping an object with a known centering offset, then checking for relative motion, as shown in Figure 10. First, the object is manually placed at a precise position on a low-friction table. Next, the hand approaches with some centering position, x_h , and attempts to grasp the object. The hand is then raised 10 mm to lift the object. Finally, the object is moved in a zig-zag pattern to determine whether any relative motion between the hand and the object occurs. For a grasp to be considered successful, the object must remain in the

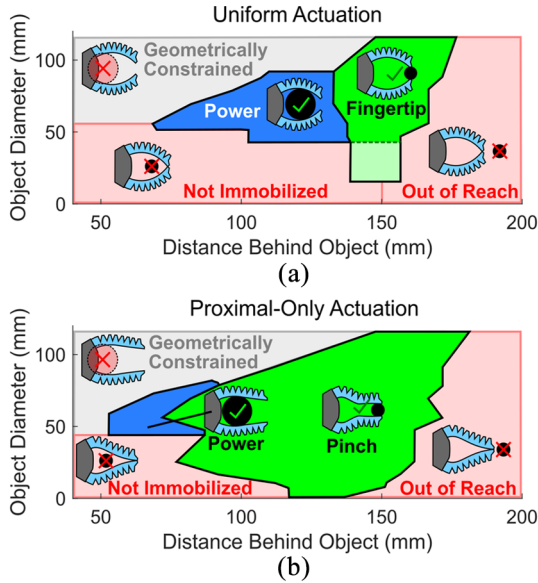


Fig. 11. Hand position and object diameter determine the type of grasp produced upon actuation, as well as failure regions. (a) For *uniform* actuation, the power grasping region is large, but only marginally stable grasps were observed for the 25 and 16 mm objects near a centering distance of 150 mm. (b) Under *proximal-only* actuation, the pinch grasping region encompasses a larger range of centering distances, and spans all the way to the thinnest object tested. All grasps were performed using fingers with equal-length segments.

same position before and after the zig-zag motion (thus, caging grasps are not considered a success in our testing).

For each successful grasp, the grasp is characterized as a power or precision grasp based on the number of contact points between the finger and object. Keeping consistent with our definitions of grasps found in Section 1, precision grasps involve one contact per finger, and power grasps involve more than one contact on at least one finger (at least three contacts total). Power grasps can also involve a large area of contact, which reduces to a line of contact between a finger and object in planar space.

The effect of centering position on grasp type was evaluated for both key actuation modes (*uniform* actuation versus *proximal-only*) over the entire range of object sizes and centering positions. Centering positions ranged from 40 to 180 mm in 5 mm increments, as measured from the front of the palm to the center of the object. In addition, each object has a limit to how close it can be placed to the palm due to geometric constraints, so testing was restricted to positions that were geometrically reachable. Results of these experiments can be found in Figure 11. In addition, a summary of the range of object diameters capable of being grasped is shown in Figure 12.

5.2. Robustness to external forces

The robustness of a grasp to applied external forces can be used as a metric to empirically evaluate the stability of a

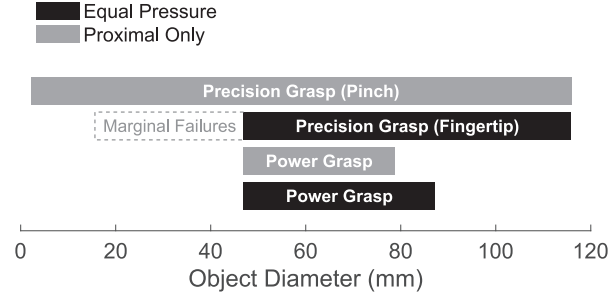


Fig. 12. Summary of successfully grasped objects for each actuation mode and grasp type using fingers with equal length segments. Under *proximal-only* actuation, the hand can grab smaller objects. The smallest grasped object is a #2-56 bolt. The dotted bar represents the size range if marginal failures were counted as successes.

grasp. Grasp robustness, as defined by Ferrari and Canny (1992), is the maximum force on the object that the gripper can resist before the object is pulled out of the hand. A minimum is taken over all possible angles the force can be applied to find the “worst-case” situation. We measured the robustness empirically by grasping an object and measuring the force required to pull it out at different angles.

For this test we used a custom-built fixture to hold the hand at angles spanning from 0° (vertical) to 90° (horizontal), as shown in Figure 3 in the Supplementary Material. The fixture allows the position and orientation of the hand to be precisely controlled with respect to the target object. The object is then pulled vertically on a uniaxial testing machine (Instron 5544A), and the force is recorded simultaneously. Neglecting the effect of gravity, this setup is equivalent to pulling an object out of the grasp at the desired angle. As a target object, we chose an acrylic cylinder with a diameter of 50.8 mm since it is in the middle of the object size range.

As mentioned in the previous section, the position of the fingers with respect to the target object defines the type of grasp performed. Using this information, we chose to test two different object positions where precision grasping and power grasping occur: at the fingertips, and at the midpoint of the fingers. Grasping under *uniform* actuation, yields fingertip grasps when the object is placed at the fingertips, and power grasps when the object is placed at the midpoint of the fingers. Grasps under *proximal-only* actuation yield pinch grasps for both object positions. We measured the force for each situation over a range of pulling angles (0°, 15°, 30°, and 45°).

5.3. Fingertip compliance during grasping

To estimate the stiffness of the finger at the contact point during a grasp, we measured the force generated by small deflections of the finger over several angles. The hand was first mounted at an angle near an Instron uniaxial testing machine using the same fixture as was used to measure



Fig. 13. Experimental setup for measuring finger stiffness while grasping, and associated schematic diagram. A single finger was actuated to perform half of a fingertip or pinch grasp on an object. Known deflections, δ , were applied to a finger at an angle θ , and the resulting force was measured. Forces applied at a desired angle were accomplished by mounting the hand at an angle, and using an Instron uniaxial testing machine to command deflections.

grasp robustness. Next, a 25.4 mm tube was positioned such that precision grasps could be performed using both modes of actuation (approximately 150 mm from the center of the palm). Only one finger was actuated against the object, forming half of a fingertip or pinch grasp, as shown in Figure 13. Finally, small deflections ranging from 1 to 5 mm were applied and the resulting increase in force was measured. Three trials for each angle were performed.

To obtain the stiffness of the finger as a function of the angle at which force was applied, the slope of the force-deflection curve was found using linear regression for each trial. The range of angles tested includes 0°, 15°, 30°, 60°, and 90° (as defined from the axis normal to the front of the palm). In addition, the small deflections of 1 to 5 mm were chosen to avoid slipping of the finger on the object. Results from these experiments are shown in Figure 14.

5.4. Relative segment lengths

To evaluate the grasping performance of fingers as a function of relative segment lengths, a subset of the tests presented above were conducted for fingers with 0.3 and 0.7 distal segment length fractions. Grasp success regions were evaluated with a subset of the objects (#2-56 bolt, 1/4-20 bolt, small marker, tube grommet, cup 1, cup 6, cup 10, and the pitcher), and robustness to external forces were measured as before. Combined with the more-detailed evaluation of fingers with equal segment lengths (0.5 distal length ratio), we aim to evaluate the trade-offs between various aspects of grasping performance as a function of segment lengths.

6. Results

The grasping performance of each set of fingers is evaluated on the basis of four metrics that can be used to compare the grasp quality and utility in a manipulation system.

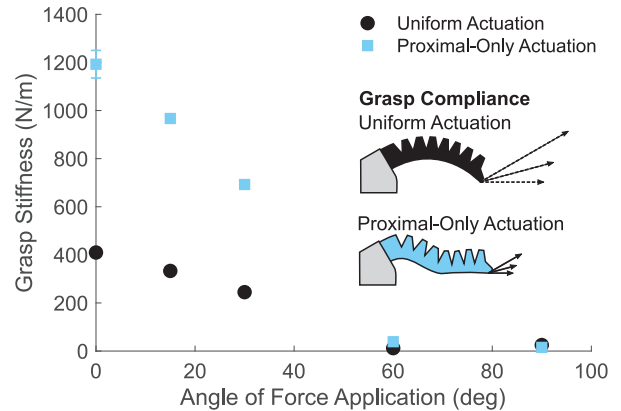


Fig. 14. Stiffness of the fingers as a function of the force application angle. The stiffness when performing a pinch grasp using *proximal* actuation is roughly three times larger than the fingertip grasps using *uniform* actuation. The diagram shows the deflection for a constant force applied at angles of 0°, 15°, and 30°. Magnitude of the vectors are exaggerated for clarity, using an equivalent of 15 N applied force. Error bars represent twice the standard deviation over $n = 3$ trials.

These metrics include a simplified estimate of the region of acquisition, an estimate of the range of object sizes that can be grasped, an estimate of the rotational stability, and the robustness to external forces on the object. In addition, the finger stiffness during grasping is characterized.

6.1. Hand placement determines grasp type

The region of acquisition describes how much error in hand position can be tolerated before it is unable to perform reliable grasps. As defined by Aukes and Cutkosky (2013), the region of acquisition is the set of all hand positions (relative to a target object) where successful grasps can occur. We empirically measured a single axis of this region along the axis of symmetry for our hand (the axis normal to the palm). In addition, we tracked how the type of grasp is affected by hand placement, allowing the formation of regions of acquisition for each grasp type and each actuation mode. The results of these experiments are shown in Figure 11.

Overall, fingers with a passive distal segment (under *proximal* actuation) can perform precision grasps over a larger range of centering distances than with *uniform* actuation. The width of the success region for pinch grasping with *proximal* actuation is three to four times the width of the fingertip grasping region with *uniform* actuation for objects in the middle of the diameter range. Furthermore, the range of centering distances that yield stable grasps increases dramatically for objects under 40 mm in diameter. In fact, the pinch grasping region for fingers under *proximal* actuation includes some objects in the smaller range that could not be grasped with *uniform* actuation.

These results follow from the geometry of the fingers during a grasp. With a passive distal segment (*proximal*

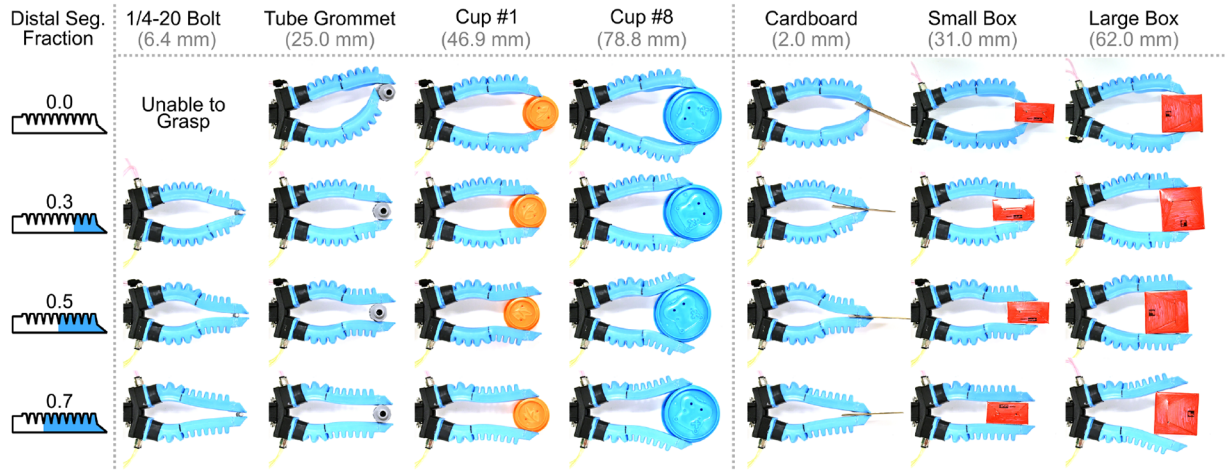


Fig. 15. Precision grasps performed on cylinders and rectangular prisms of a variety of widths. The general shape of the fingers during grasping is relatively constant for each object as the distal segment length fraction decreases from 0.7 to 0.3. However, a fundamental difference in shape occurs for 0.0 (no distal segment) compared to fingers with distal segments.

actuation), the object can be grasped anywhere along the distal segment, whereas contact points are limited to only the fingertips when using *uniform* actuation. Thus, we would expect a drastic increase in the size of the pinch-grasping region because the passive distal segment can grasp in positions that could only be caged using *uniform* actuation.

Conversely, fingers under *uniform* actuation can perform power grasps over a larger range of centering distances. The power grasping region for *proximal* actuation appears to shrink by approximately 70% on average for larger objects. This makes sense because much of the centering distances where power grasps are performed with *uniform* actuation result in pinch grasps with *proximal* actuation.

In addition, geometric considerations can explain the failure regions. For example, all grasps fail in the region beyond 160 mm centering distance, as this is beyond the reach of the fingers. In addition, some regions were unable to be tested due to geometric constraints. For objects 47 mm and larger, the empty region to the left of the power grasping region is physically impossible to test.

One special case for our finger design involves fingertip grasps on small objects using *uniform* actuation. For small objects (25 and 16 mm), rolling instabilities on the fingertips can cause marginally stable grasps that snap to one side or the other. This forms grasps where the object is in contact with the fingertip of one finger and the back side of the other finger. An example of this type of grasp is shown in Figure 15 for fingers with distal segment length fraction of 0.0 grasping a tube grommet. For the purposes of this analysis, we consider these types of grasps as marginal failures, since the final object pose is not predictable.

Finally, it is important to note that for the small objects that could not be grasped by fingers under *uniform* actuation, failures involved rotational instability. All failures for

objects smaller than 16 mm around an approximately 150 mm centering offset involved the fingertips applying force slightly off-center due to small differences in actuator performance. This slight off-center force balance caused the object to undergo large rotations, and thus large fingertip motions, eventually pushing the object out of the grasp.

6.2. Object size range

The range of object sizes capable of being stably grasped is another metric we can use to evaluate the effect of additional bending segments in our soft fingers. We can extract this metric from the results of the experiments performed in the previous section by identifying the largest and smallest objects that could be grasped for a given grasp type and actuation mode. A summary of the range of diameters that can be successfully grasped using each combination of actuation modes and grasp types are shown in Figure 12.

According to our measurements, the upper bound on object size is similar regardless of the actuation mode or type of grasp. Overall, the largest possible object that can be grasped is 116 mm in diameter. This makes sense because we expect the upper bound to be limited by hand geometry.

When operating with *uniform* actuation, a lower bound on object size exists. The smallest object that was successfully grasped is 16 mm in diameter, but this occurs only when performing a marginally stable fingertip grasp. In this case, fingertip grasping is necessary because the diameter of the object is smaller than the minimum diameter that can be power grasped. The lower bound makes sense because fingertip grasp stability is a function of the object and fingertip curvatures, making grasps on smaller objects unstable.

Alternatively, when operating with a passive distal segment (*proximal* actuation), the lower bound on object size

appears to be arbitrarily small. Successful pinch grasps were capable of being performed on arbitrarily thin objects (such as a sheet of paper). This is due to the fact that the point of contact with objects is on the inside of the finger, and the passive distal segment can bend backward to achieve approximately zero curvature (flat plate). Thus, grasps are kinematically stable regardless of object diameter according to Cutkosky and Wright (1986), and are instead limited by contact forces.

Overall, the results presented in the last two sections represent fundamental performance tradeoffs arising from finger structure. It is clear that having a passive distal segment (with the proximal segment actuated) is directly responsible for better functionality compared to fingers with one uniformly actuated bending segment. Fingers with one uniform bending segment are unable to grasp objects below some minimum diameter due to rotational instability. However, fingers with passive distal segments can achieve stable pinch grasps on arbitrarily thin objects without affecting the maximum possible diameter.

6.3. Rotational stability

Rotational stability plays a large role in the overall success of precision grasps. We can observe the effects of rotational stability (or instability) on grasps by tracking the object's pose over time. For both actuation modes, the position and orientation of a small object was tracked as a precision grasp was attempted. The positions of contact points were tracked manually for each frame in the videos using Tracker Video Analysis and Modeling Software (Tracker, 2019) as described in the Supplementary Material. The results are shown in Figure 16.

It can be clearly seen from the motion of the *object that the rotational stability of a fingertip grasp under *uniform* actuation is lower than that of a pinch grasp under *proximal-only* actuation. During the grasp attempt, the object's pose changes rapidly, with the angle of the object changing by 60° from the starting position. This is due to rotation between the fingertip and the object. In contrast, the object neither moves nor rotates at all when a pinch grasp is performed with *proximal* actuation. This is because the object is grasped on the inside edge of the flat segment, so object rotation cannot occur unless the object slips with respect to the finger.

6.4. Robustness to external forces

Robustness to external forces is critical for maintaining a grasp once it is successful. To understand how the grasp robustness differs for different actuation modes and grasp types, we look at the results of the pull force tests displayed in Figure 17.

It turns out that when a grasp occurs at the fingertip, grasping under *uniform* actuation shows a greater average resistance to forces applied to the object compared to pinch grasping with *proximal* actuation. However, when the

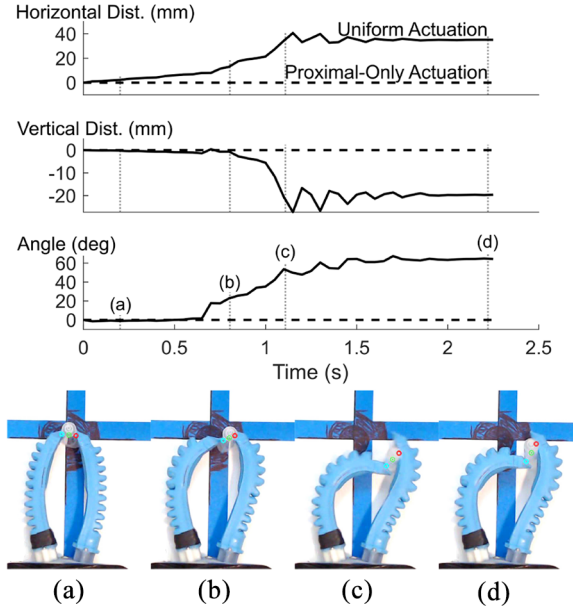


Fig. 16. Rotational instability during a fingertip grasp causes large object rotation and translation. Pictures correspond to time points in the graphs as marked. The object grasped was a 16 mm syringe.

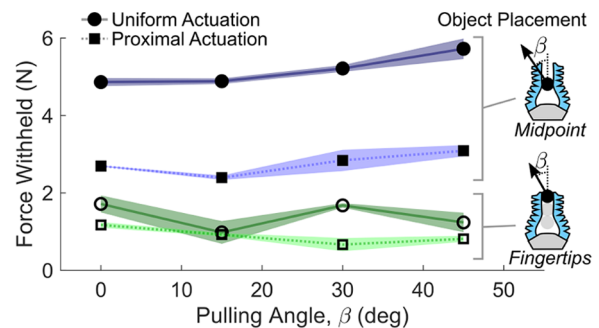


Fig. 17. The average minimum force to pull out a 50.8 mm cylinder for different grasps using fingers with equal-length segments. Error bars represent one standard deviation over $n = 3$ runs.

cylinder is placed deeper in the pinch grasp, the pull-out force is on average 96% higher than a fingertip grasp using *uniform* actuation. When it comes to a power grasp using *uniform* actuation, the required force is significantly higher (5.17 N on average over all angles). In all four situations, the angle (in this range) does not appear to be a consistent factor leading to any significant change in the pull force.

As before, these results using the two actuation modes are indicative of the performance of the two fundamental finger structures we are studying. These results indicate that if an object is large enough to be power grasped, fingers with a single uniformly actuated segment perform far better than fingers with two segments where the distal segment is passive. However, when an object is too small to be power

grasped, fingertip grasping with single-segment uniformly actuated fingers performs better than pinch grasping with passive distal segments. Finally, if the object is too small to be grasped with uniformly actuated fingers, pinch grasps using fingers with a passive distal segment are more robust as the object is placed deeper in the grasp.

6.5. Grasp stiffness

Overall, the finger stiffness during grasping was higher with two-segment fingers than with single-segment fingers. The results of these experiments are shown in Figure 14. At 0° (aligned with the axis of symmetry), the stiffness of the finger under *uniform* actuation is $410 \pm 30 \text{ N m}^{-1}$. Meanwhile, the pinch-grasping stiffness for fingers under *proximal-only* actuation is $1,200 \pm 110 \text{ N m}^{-1}$. For angles of 0° , 15° , and 30° , the finger with a passive distal segment had a stiffness on average 2.9 times that of the single-segment finger. The variability in stiffness measurements was on the order of 8–9% at 0° , and less than 2% at all other angles. Interestingly, stiffnesses were much lower for both finger designs at more extreme angles of 60° and 90° .

6.6. Relative length of finger segments

To evaluate the effect of relative segment lengths on grasping performance, we performed hand placement and grasp robustness tests on two additional length ratios (0.3 and 0.7 distal length fraction) under *proximal-only* actuation. The results of these tests can be directly compared to the original fingers with equal segment lengths (0.5 distal length fraction) under *proximal-only* actuation. In addition, fingers with equal segment lengths can simulate the performance of similar fingers with one uniformly actuated bending segment (0.0 distal length fraction) when actuated with *uniform* pressure. Representative samples of the resulting grasps for some of the objects tested are shown in Figure 15.

From a geometric standpoint, the region of grasp success transitions from mostly power grasps to entirely precision grasps as the relative length fraction of the distal segment (distal segment fraction) increases, as shown in Figure 18. With a distal segment fraction of 0.0, power grasping occurs when the palm is between 70 and 135 mm behind the object, and precision grasping occurs between 135 mm and 170 mm. By contrast, fingers with a distal segment ratio of 0.7 exhibit no power grasping region, and precision grasps occur between 60 mm and 165 mm behind the object. In addition, increasing the distal segment length increases the range of successful hand positions for smaller objects.

Our experiments evaluating the forces during grasping show the grasp robustness generally decreases as the distal segment length fraction increases, as shown in Figure 19. Robustness was tested with objects placed at the midpoint of the fingers and at the fingertips. In both cases, the minimum force withheld appears to decrease as a function of

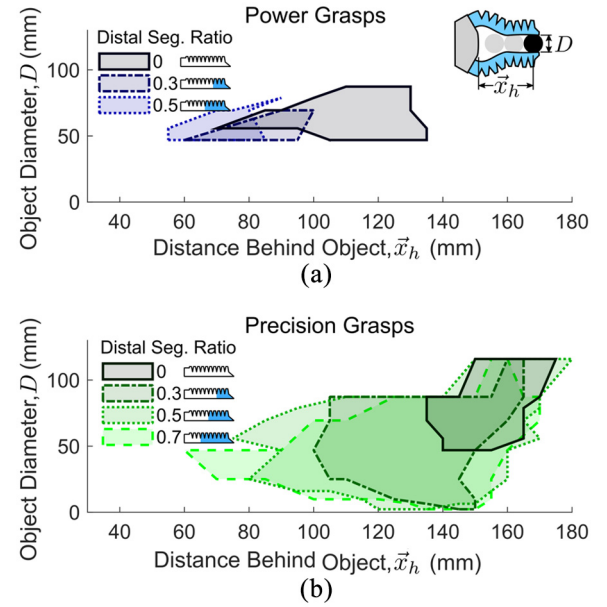


Fig. 18. The relative lengths of finger segments affect which grasp types are successful under proximal-only actuation. (a) The power grasp region appears to shrink as the length of the distal finger segments increases (relative to overall finger length). In fact, a distal segment ratio of 0.7 exhibits no power-grasping region at all. (b) Conversely, the precision grasp region appears to expand as the distal segment length increases. Shaded regions represent successful grasps.

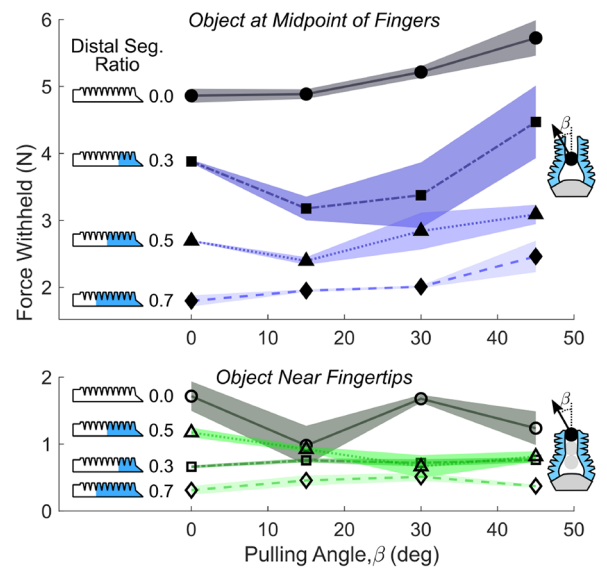


Fig. 19. The relative lengths of finger segments affect the grasp robustness under proximal-only actuation for two different object placements. With the object at the midpoint of the fingers, grasps are overall stronger (more robust) with a length ratio of 0.0 providing the most robust grasps. With the object near the fingertips, grasps are overall weaker (less robust) with the length ratio of 0.7 being the least robust. In both cases, the minimum force withheld generally decreases as the distal length increases. Grasps were performed on a 50.4 mm cylinder, and shaded regions represent the standard deviation in the force withheld over $n = 3$ trials.

the distal segment fraction. This relationship appears distinct when the object is placed at the midpoint of the fingers, while the robustness of fingertip grasps is similar for all distal segment fractions tested. In addition, grasps on the object at the midpoint of the fingers are overall stronger than with the object placed at the fingertips. This makes sense due to the larger lever arm over which contact forces are transmitted, and the shorter actuated proximal segment as the distal segment length increases.

6.7. Grasping arbitrary objects

In addition to cylindrical objects, we tested grasps on rectangular prisms of varying thicknesses from 2 mm (cardboard sheet) to 60 mm (a square box). In all cases, prisms were placed with the sides parallel to the axis of symmetry of the hand. Representative samples of the resulting grasps are shown in Figure 15. As expected, the shapes of fingers during grasping are not substantially different from grasps performed on cylindrical objects of similar width. In addition, the results of hand position tests for this set of rectangular prisms are shown in Figure 20.

In addition to similar finger shapes during grasps, the stability of precision grasps on thin objects (judged by examining the amount of extraneous object motion during the initial grasp) is still increased when using fingers with a passive distal segment as compared to no distal segment. For example, grasping a thin plate with no distal segment causes large object rotation owing to the small radius of curvature of the fingertips. Conversely, grasping with fingers that have passive distal segments causes minimal object motion. This is the same trend as was observed with cylinders.

While the benefit of a passive distal segment on grasp stability is similar for prisms and cylinders, the success region for fingers with no distal segment is substantially improved for small objects. Using fingers with no distal segment, a 2 mm thick cardboard sheet is easily grasped. This is due to the aid of a third contact point at one of the fingers. In addition, the radius of curvature of the cardboard sheet near the fingertips is large (essentially infinite), and the distance between contacts is small, leading to higher rotational stability compared to a cylinder with a similar diameter.

The other main difference in grasping rectangular prisms vs. cylinders is that precision grasps are successful over a much larger range of hand centering positions, as shown in Figure 20. This is because the precision-grasping region for rectangular shapes extends for the entire length of the object, whereas precision grasps are often not successful for cylinders until the fingertips pass the midpoint of the object. The opposing sides of rectangular prisms are best grasped by parallel forces from the fingers, which can be generated robustly by fingers that have a distal segment (distal segment fractions greater than 0.0). In this way, these fingers behave similar to a parallel-jaw gripper.

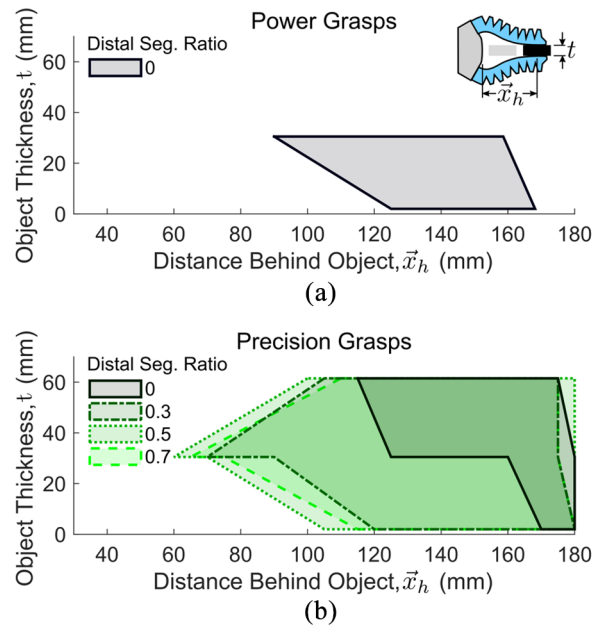


Fig. 20. Grasping rectangular prisms does not substantially change grasping performance compared to cylindrical objects. (a) Due to object geometry, only fingers with a distal segment ratio of 0 were capable of power grasps on the rectangular prisms tested. (b) The range of centering distances that result in successful precision grasps is larger for smaller objects compared to similarly sized cylinders.

7. Discussion

In this section, we analyze the results of the grasp performance characterization from above. In addition to confirming the proposed high-level design principles, we also confirm the reasoning behind them, and discuss performance tradeoffs that arise. We then generalize our results to arbitrary objects, since we expect trends to remain similar regardless of object geometry. Finally, we discuss how our results can be generalized to grasping in three dimensions.

7.1. Two-segment fingers enable robust pinch grasps

Based on three of the four grasping metrics, the precision grasping capabilities of a soft finger can be drastically improved using two bending segments with only the proximal segment actuated. For our prototype soft fingers, the only way to successfully grasp small objects below 16 mm in diameter is to perform a pinch grasp using *proximally actuated* fingers. In addition, for the entire range of objects, a pinch grasp using a two-segment finger design had a much larger range of centering positions where successful grasps could be performed. The larger region of success for pinch grasping makes the hand much less sensitive to positioning errors compared to using fingertip grasps (with one-segment fingers). The rotational stability of pinch grasps is also higher owing to the much smaller finger

curvature at the contact points. Finally, while the grasp robustness of pinch grasps was lower than fingertip grasps, the difference was small compared to the magnitude of forces applied.

Overall, the benefit of designing soft fingers with a passive distal segment (or similar compliant mechanism at the fingertip) is clear. Using soft fingers with one uniform segment, a hand can only perform precision grasps with the fingertips. However, the two-segment structure enables pinch grasping, which has a higher utility than fingertip grasping when fingers are highly compliant.

7.2. Power grasps are better-performed with one uniform segment

Based on the grasp robustness measurements, power grasping is better-performed with a single uniformly actuated segment than with two-segment fingers with passive distal segments. First, the power grasping region is very small when using a two-segment structure with a passive distal segment compared to single uniformly actuated segment, so there are less opportunities to perform a power grasp. In most cases, power grasping is simply not possible with our two-segment finger design.

In addition, the robustness of power grasping with fingers that have one uniformly actuated segment is much higher than that of pinch grasping with a passive distal segment, even in the best case. The best pinch grasping performance occurs when the object is deeper in the grasp. However, the minimum pull-out force for a power grasp using a single uniformly actuated segment was approximately 150% higher than for a pinch grasp with a passive distal segment. Thus, for our soft hand, the best power grasping performance requires a single uniformly actuated bending segment.

7.3. Performance tradeoffs inform design of segment lengths

While it is clear that fingers with passive distal segments enable more stable precision grasping, our exploration of the relative lengths of finger segments suggests that a fundamental tradeoff exists between grasp robustness and precision grasp stability. Some optimal ratio of segment lengths exists, however the solution is likely dependent on the detailed design of the fingers and task requirements, and would undoubtedly require compromises in performance. An understanding of tradeoffs in performance space is therefore critical during the design process.

From our investigation, it is clear that precision grasping is necessary to grasp smaller objects, but this can only be achieved robustly with continuum fingers if a passive distal segment (or similar compliant fingertip structure) is employed. As shown in Figure 18, fingers with no distal segment are unable to produce stable grasps on smaller objects, while even a small passive distal segment (0.3

distal length fraction) enables grasping arbitrarily small objects. Furthermore, the size of the precision grasping region increases as the distal length ratio increases, as shown in Figure 18. This means that grasps can be performed over a larger range of hand positions on smaller objects with a larger distal segment fraction.

Conversely, power grasping is clearly the strongest grasping mode for larger objects, but the robustness (ability to withstand pull-out forces) of power grasps diminishes as the passive distal segment is lengthened. In fact, the power grasp robustness is highest when the finger has no distal segment (distal length ratio of 0.0). However, with a short distal segment (length fraction of 0.3), the minimum force withheld by power grasps is 35% smaller than with no distal segment.

From this investigation, we can draw the conclusion that some local optimum exists where the grasping region extends down to arbitrarily small objects while minimally affecting power grasp robustness. However, a more thorough understanding of the shape of this performance space would be needed before an optimal ratio of segment lengths can be determined for any particular application.

7.4. Two independently actuated segments enable best performance

Based on the discussion thus far, it is clear that a hand with soft, continuum fingers can only achieve the best possible grasping performance during both power grasps and pinch grasps by using two different finger structures. The most-robust power grasps occur using fingers with a single uniformly actuated bending segment. On the flip side, the most-successful precision grasps occur during pinch grasping, which requires two bending segments with only the proximal segment actuated.

Using two actuated segments in each finger enables on-the-fly adaptation between both desired finger structures with only a small increase in control complexity. As shown in this article, fingers with two independently actuated segments can replicate the performance of both fundamental soft finger structures. Thus, through control of both finger segments, we can achieve the best grasping performance of both structures.

7.5. Fingertip compliance and shape

According to our experimental investigation, we have corroborated the conceptual design analysis presented in Section 2. Fingertip compliance and local shape clearly play a role in the stability of grasps performed by soft robotic fingers. In addition, these features were tracked for both the one-segment and two-segment finger structures, and can be used to explain trends in stability.

First, the stability of fingertip grasps is very low when using a single bending segment, since all of the failed attempts to grasp smaller objects were caused by fingertip

rolling instabilities. The rolling instabilities are caused by the extremely small radius of curvature of the fingertips used in our prototype system. Conversely, the range of successfully grasped diameters was extended down to zero when using pinch grasps with two bending segments. This is due to increased rotational stability gained when grasping with flat contacts on the side of the finger.

Next, the compliance of the fingers during a pinch grasp is smaller in the axis normal to the palm's surface compared to a fingertip grasp. Thus, not only are rolling instabilities mitigated, but the amount of finger deflection per unit force on the object is smaller.

Overall, our experiments clearly demonstrate that consideration of simple design attributes can be used to explain why two independently controlled bending segments (or similar compliant fingertip structures) in soft robotic fingers are fundamentally necessary. Through increased rotational stability due to low curvature at the contact point, pinch grasps enable soft fingers to grasp smaller objects, and are more robust against small perturbations. In addition, two-segment fingers can control object motion to a higher degree through increased stiffness. All of these capabilities can lead to important functions in real use cases.

7.6. Grasping arbitrary objects

In the real world, robots need to be capable of interacting with a variety of object shapes. Rarely do robots encounter perfect cylinders or prisms in two dimensions. To understand the changes in performance when grasping arbitrary objects, we can turn back to the stability analysis of Cutkosky and Wright (1986). For any arbitrary object, we can break down a grasp on that object into local object curvature near the contacts and the distance between contact points. In our experiments with cylindrical objects, the object curvature and distance between contacts are coupled by geometry. However, in general these two parameters are decoupled. This decoupling leads to potentially far better grasping performance if the object is thin and flat at the contact points, and far worse performance if the object is thick and rounded at the contacts.

Based on this analysis, we would expect the stability of any grasp to increase as the object curvature decreases (as the sides of the object become flatter). Coupled with the ability to passively enable parallel finger segments, we would expect the increase in grasp stability for soft fingers with two segments versus one segment to be even more drastic. In our study, we confirm this trend by the fact that grasps could be performed on arbitrarily thin rectangular prisms using fingers with no distal segment, whereas grasps on cylinders with the same finger structure had a lower bound on object size that could be grasped successfully.

Overall, the design principles laid out in this work for how to utilize multi-segment continuum fingers for pinch grasping appear to generalize to a wide variety of object shapes. While complicated shapes may change the magnitudes of the trends found in this study, we expect the

general trends to remain similar. As we showed in our comparison of cylinders versus rectangular prisms, the shapes of fingers during grasping were similar for similarly sized objects. In addition, a general increase in the stability of precision grasps when using passive distal segments also remained true regardless of object shape. Based on this evaluation, we expect the fundamental design principles discussed in this article to remain similar for arbitrary objects.

7.7. Extension to non-planar grasping

In addition to arbitrary objects, real-life manipulation tasks involve moving objects in six dimensions (translations and rotations about all three axes). While our analysis and experimental validation of finger design was performed for the planar case, we can extend our results directly to real-world conditions in two important cases.

One simple extension involves using a planar hand to perform antipodal grasps, but moving the object in 3D space. Antipodal grasps are commonly performed in robotic manipulation. If the off-axis stiffness of soft fingers is high enough, grasping can be performed in a plane with minimal fingertip deviation, and translations and rotations in 3D space become trivial, as shown in Figure 21 and Supplemental Video S1. In this case, the finger design rules presented in this study can be directly used to build a robust antipodal gripper.

Finally, we also expect our results to apply to grippers with radial symmetry. With fingers arranged radially, pinch grasps on axisymmetric target objects would be functionally similar to pinch grasps performed by our planar hand. Overall, we expect the analysis and empirical results of this study to remain structurally similar for object motion in 3D space.

8. Conclusions and future work

We explored how simple design rules can produce soft robotic fingers capable of excellent precision grasping without sacrificing power-grasping performance. We presented and validated a conceptual analysis of grasping using soft fingers with multiple serially linked bending segments. Through this analysis and an extensive empirical investigation, we showed that designing different finger structures for each grasp type clearly outperforms any single finger structure. We found that pinch grasps have increased stability compared to fingertip grasps, and achieving pinch grasps requires fingers with at least two bending segments, though only the proximal segment needs to be actuated. Further, we showed that robust power grasping requires fingers with one uniformly actuated bending segment. Based on this investigation, we showed that fingers with two independently actuated segments can gain the best functionality of both finger structures through a small increase in control complexity. Finally, we demonstrate the necessity of online choice between power and

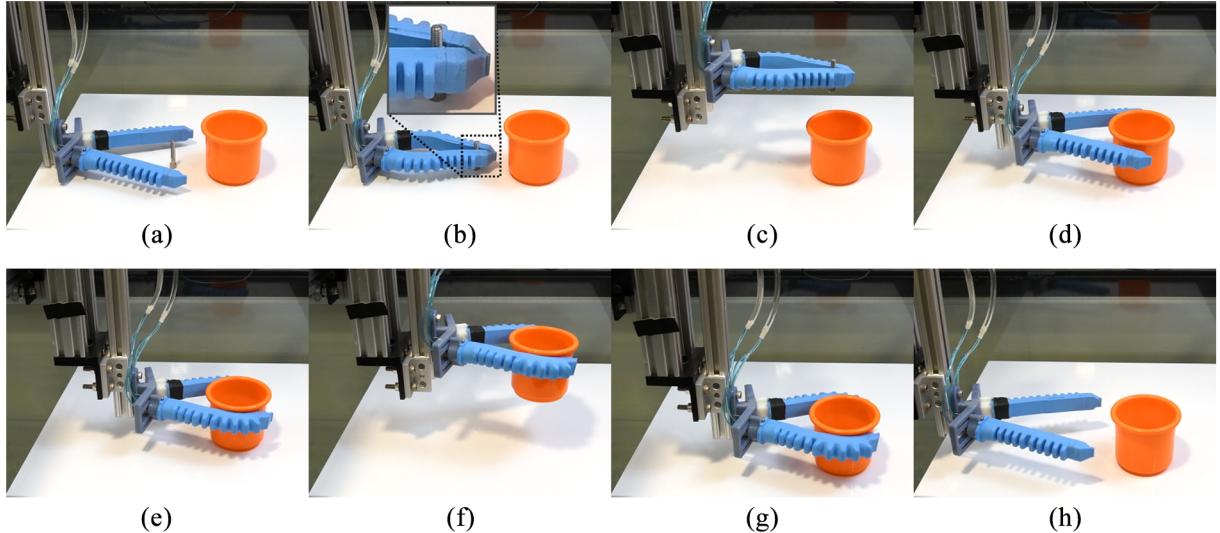


Fig. 21. Online adaptation between pinch grasps and power grasps is essential for grasping tasks involving objects of small and large sizes. This is illustrated by the task of placing a bolt of 6 mm diameter into a large cup of 80 mm, then moving the cup. (a)–(d) Due to the bolt’s small size, a pinch grasp must be performed to move it to the cup. (e), (f) After releasing the bolt, the hand performs a power grasp on the cup. (g)–(j) Finally, the cup is moved to a new position and released.

precision grasps during a pick-and-place operation, and discuss extensions of our work to arbitrary objects and non-planar manipulation.

Nonetheless, there remains potential for future work exploring the capabilities of these multi-segmented soft fingers. The benefits of intrinsic compliance become most-relevant when soft actuators are dealing with fragile objects, or targets with complex morphologies. Furthermore, the design concepts presented here could be further refined by exploring finger designs with non-uniform stiffness. Extending hands beyond planar configurations to explore 3D grasps using soft, two-segment fingers is also a natural next step.

In addition to the mechanical design of two-segment soft fingers, mathematical models and sensory feedback could enable finer tuning of grasps, or even in-hand manipulation. Models of finger deformation under contact could be used as a design tool, or to aide in the generation of grasping strategies. On-board shape estimation could provide insight into how local deformations lead to successful grasps. Contact sensing could improve the sensitivity of pinch grasps, and potentially enable success estimation without the need for external vision systems. Overall, the work in this article sets the stage for high-quality grasping using soft robotic hands.

Acknowledgments

The authors would like to thank Kaitlyn Becker, Michael Bell, Daniel Vogt, and Thibaut Paschal for essential discussions on soft robot fabrication, and Patrick Varin for helpful discussions about grasp stability.

Funding

This work was supported by the National Science Foundation (NSF EFRI award number 1830901, NSF IDBR award number 1556164, and NSF Graduate Research Fellowship award number DGE1745303). Any opinions, findings, and conclusions or recommendations expressed in this material are those of the authors and do not necessarily reflect the views of the National Science Foundation.

References

- Amend J and Lipson H (2017) The JamHand: Dexterous manipulation with minimal actuation. *Soft Robotics* 4(1): soro.2016.0037.
- Aukes DM and Cutkosky MR (2013) Simulation-based tools for evaluating underactuated hand designs. *2013 IEEE International Conference on Robotics and Automation (ICRA)*, pp. 2067–2073.
- Aukes DM, Heyneman B, Ulmen J, et al. (2014) Design and testing of a selectively compliant underactuated hand. *The International Journal of Robotics Research* 33(5): 721–735.
- Bae JH, Park SW, Park JH, Baeg MH, Kim D and Oh SR (2012) Development of a low cost anthropomorphic robot hand with high capability. In: *2012 IEEE/RSJ International Conference on Intelligent Robots and Systems*. IEEE, pp. 4776–4782.
- Bridgwater LB, Ihrke C, Diftler MA, et al. (2012) The robonaut 2 hand-designed to do work with tools. In: *2012 IEEE International Conference on Robotics and Automation*. IEEE, pp. 3425–3430.
- Brown E, Rodenberg N, Amend J, et al. (2010) Universal robotic gripper based on the jamming of granular material. *Proceedings of the National Academy of Sciences* 107(44): 18809–18814.

- Bullock IM, Zheng JZ, De La, Rosa S, Guertler C and Dollar AM (2013) Grasp frequency and usage in daily household and machine shop tasks. *IEEE Transactions on Haptics* 6(3): 296–308.
- Butterfaß J, Grebenstein M, Liu H and Hirzinger G (2001) DLR-Hand II: Next generation of a dexterous robot hand. In: *Proceedings 2001 IEEE International Conference on Robotics and Automation (ICRA)*, Vol. 1. IEEE, pp. 109–114.
- Calli B, Walsman A, Singh A, Srinivasa S, Abbeel P and Dollar AM (2015) Benchmarking in manipulation research: Using the Yale–CMU–Berkeley object and model set. *IEEE Robotics & Automation Magazine* 22(3): 36–52.
- Catalano MG, Grioli G, Farnioli E, Serio A, Piazza C and Bicchi A (2014) Adaptive synergies for the design and control of the pisa/iit softhand. *The International Journal of Robotics Research* 33(5): 768–782.
- Chitta S, Sucan I and Cousins S (2012) Moveit! [ROS Topics]. *IEEE Robotics Automation Magazine* 19(1): 18–19.
- Ciocarlie M, Hicks FM, Holmberg R, et al. (2014) The Velo gripper: A versatile single-actuator design for enveloping, parallel and fingertip grasps. *The International Journal of Robotics Research* 33(5): 753–767.
- Cutkosky MR (1989) On grasp choice, grasp models, and the design of hands for manufacturing tasks. *IEEE Transactions on Robotics and Automation* 5(3): 269–279.
- Cutkosky MR and Wright PK (1986) Friction, stability and the design of robotic fingers. *The International Journal of Robotics Research* 5(4): 20–37.
- De A and Tasch U (1996) A two-dof manipulator with adjustable compliance capabilities and comparison with the human finger. *Journal of Robotic Systems* 13(1): 25–34.
- Deimel R and Brock O (2013) A compliant hand based on a novel pneumatic actuator. In: *2013 IEEE International Conference on Robotics and Automation*. IEEE, pp. 2047–2053.
- Deimel R and Brock O (2016) A novel type of compliant and underactuated robotic hand for dexterous grasping. *The International Journal of Robotics Research* 35(1–3): 161–185.
- Deimel R, Irmisch P, Wall V and Brock O (2017) Automated co-design of soft hand morphology and control strategy for grasping. In: *2017 IEEE/RSJ International Conference on Intelligent Robots and Systems (IROS)*. IEEE, pp. 1213–1218.
- Dollar AM and Howe RD (2010) The highly adaptive SDM hand: Design and performance evaluation. *The International Journal of Robotics Research* 29(5): 585–597.
- Feix T, Pawlik R, Schmiedmayer HB, Romero J and Kragic D (2009) A comprehensive grasp taxonomy. In: *Robotics, Science and Systems: Workshop on Understanding the Human Hand for Advancing Robotic Manipulation*, Vol. 2, pp. 2–3.
- Ferrari C and Canny J (1992) Planning optimal grasps. In: *Proceedings 1992 IEEE International Conference on Robotics and Automation*. IEEE, pp. 2290–2295.
- Friedl W, Höppner H, Schmidt F, Roa MA and Grebenstein M (2018) CLASH: Compliant low cost antagonistic servo hands. In: *2018 IEEE/RSJ International Conference on Intelligent Robots and Systems (IROS)*. IEEE, pp. 6469–6476.
- Galloway KC, Becker KP, Phillips B, et al. (2016) Soft robotic grippers for biological sampling on deep reefs. *Soft Robotics* 3(1): soro.2015.0019.
- Gravagne IA and Walker ID (2002) Manipulability, force, and compliance analysis for planar continuum manipulators. *IEEE Transactions on Robotics and Automation* 18(3): 263–273.
- Hajian AZ and Howe RD (1997) Identification of the mechanical impedance at the human finger tip. *Journal of Biomechanical Engineering* 119: 109–114.
- Hogan N (1985) Impedance control: An approach to manipulation: Part II - implementation. *Journal of Dynamic Systems, Measurement, and Control* 107(1): 8–16.
- Hughes J, Culha U, Giardina F, Guenther F, Rosendo A and Iida F (2016) Soft manipulators and grippers: A review. *Frontiers in Robotics and AI* 3: 69.
- Ilievski F, Mazzeo AD, Shepherd RF, Chen X and Whitesides GM (2011) Soft robotics for chemists. *Angewandte Chemie* 123(8): 1930–1935.
- Jacobsen S, Iversen E, Knutti D, Johnson R and Biggers K (1986) Design of the Utah/MIT dexterous hand. In: *Proceedings. 1986 IEEE International Conference on Robotics and Automation*, Vol. 3. IEEE, pp. 1520–1532.
- Knoop E, Bächer M, Wall V, Deimel R, Brock O and Beardsley P (2017) Handshakiness: Benchmarking for human–robot hand interactions. In: *2017 IEEE/RSJ International Conference on Intelligent Robots and Systems (IROS)*. IEEE, pp. 4982–4989.
- Kochan A (2005) Shadow delivers first hand. *Industrial Robot: An International Journal* 32(1): 15–16.
- Lim HO and Tanie K (2000) Human safety mechanisms of human-friendly robots: Passive viscoelastic trunk and passively movable base. *The International Journal of Robotics Research* 19(4): 307–335.
- Majidi C (2014) Soft robotics: A perspective — current trends and prospects for the future. *Soft Robotics* 1(1): 5–11.
- Maruyama R, Watanabe T and Uchida M (2013) Delicate grasping by robotic gripper with incompressible fluid-based deformable fingertips. *IEEE International Conference on Intelligent Robots and Systems* : 5469–5474.
- McInroe BW, Chen CL, Goldberg KY, Bajcsy R and Fearing RS (2018) Towards a soft fingertip with integrated sensing and actuation. In: *2018 IEEE/RSJ International Conference on Intelligent Robots and Systems (IROS)*. pp. 6437–6444.
- Montana DJ (1992) Contact stability for two-fingered grasps. *IEEE Transactions on Robotics and Automation* 8(4): 421–430.
- Morrow J, Shin HS, Phillips-Grafflin C, et al. (2016) Improving Soft Pneumatic Actuator fingers through integration of soft sensors, position and force control, and rigid fingernails. In: *2016 IEEE International Conference on Robotics and Automation (ICRA)*, pp. 5024–5031.
- Mussa-Ivaldi F, Hogan N and Bizzi E (1985) Neural, mechanical, and geometric factors subserving arm posture in humans. *The Journal of Neuroscience* 5(10): 2732–2743.
- Odhner LU, Jentoft LP, Claffee MR, et al. (2014) A compliant, underactuated hand for robust manipulation. *The International Journal of Robotics Research* 33(5): 736–752.
- O'Brien KW, Xu PA, Levine DJ, et al. (2018) Elastomeric passive transmission for autonomous force-velocity adaptation applied to 3D-printed prosthetics. *Science Robotics* 3(23): eaau5543.
- Polygerinos P, Correll N, Morin SA, et al. (2017) Soft robotics: Review of fluid-driven intrinsically soft devices; manufacturing, sensing, control, and applications in human-robot interaction. *Advanced Engineering Materials* 19(12): 1700016.
- Quigley M, Conley K, Gerkey BP, et al. (2009) ROS: An open-source robot operating system. In: *ICRA Workshop on Open Source Software*.
- Robotiq (2019) 2f-85 and 2f-140 grippers. *Online datasheet*. Available at: <https://robotiq.com/products/2f85-140-adaptive-robot-gripper>.

- Rus D and Tolley MT (2015) Design, fabrication and control of soft robots. *Nature* 521(7553): 467.
- Shintake J, Cacucciolo V, Floreano D and Shea H (2018) Soft robotic grippers. *Advanced Materials* 30(29): 1707035.
- Townsend W (2000) The Barretthand grasper-programmably flexible part handling and assembly. *Industrial Robot: An International Journal* 27(3): 181–188.
- Tracker (2019) Tracker Video Analysis and Modeling Software, version 5.0.7. Available at: <https://physlets.org/tracker>
- Vogt DM, Becker KP, Phillips BT, et al. (2018) Shipboard design and fabrication of custom 3D-printed soft robotic manipulators for the investigation of delicate deep-sea organisms. *PLoS ONE* 13(8): e0200386.
- Zhou J, Chen S and Wang Z (2017) A soft-robotic gripper with enhanced object adaptation and grasping reliability. *IEEE Robotics and Automation Letters* 2(4): 2287–2293.
- Zhou J, Yi J, Chen X, Liu Z and Wang Z (2018) BCL-13: A 13-DOF soft robotic hand for dexterous grasping and in-hand manipulation. *IEEE Robotics and Automation Letters* 3(4): 3379–3386.